Confined Vortex Flows with Boundary-Layer Interaction

M. L. Rosenzweig,* W. S. Lewellen,† and D. H. Ross‡
Aerospace Corporation, Los Angeles, Calif.

Axisymmetric flow of an incompressible fluid in a right-cylindrical vortex tube bounded by planar end walls is considered. The mutual interaction of the primary vortex flow field and the end-wall boundary layers is studied by relating the stream function and circulation in these regions. An interaction parameter is defined which determines the magnitude of the influence of the boundary layers on the circulation and mass-flow distributions in the primary flow. These distributions are obtained numerically, primarily as functions of the interaction parameter and the Reynolds number based on the radial flow. Experimental results are interpreted in the light of this theory, and it is concluded that substantial turbulence levels (though somewhat less than estimates made without consideration of boundary-layer effects) must be assumed to explain the experimental results.

Nomenclature

A = boundary-layer interaction parameter defined in Eq. (17)
c = coefficient of friction
F = dimensionless part of the stream function that is independent of z
f = dimensionless part of the stream function that is linear with z
l = length of the vortex chamber
p = pressure
Q = volume flow per unit length, ur
Q_{BL} = volume flow in the end-wall boundary layer
Re_r = radial Reynolds number = $\rho ur/\mu$
$Re_r{}^*$ = "effective" turbulent radial Reynolds number
Re_t = tangential Reynolds number = $\rho vr/\mu$
r = radial coordinate
u = radial velocity, positive outward
v = tangential velocity
w = axial velocity
z = axial coordinate
α = velocity-profile shape parameter in the boundary layer
Γ = circulation, vr
δ = end-wall boundary-layer thickness
ϵ = dimensionless parameter defined in Eq. (5)
η = dimensionless radial coordinate squared
μ = viscosity
ν = kinematic viscosity
ξ = dimensionless axial coordinate
ρ = density
ψ = stream function defined in Eq. (7)

Subscripts

0 = value at outer edge of the vortex tube
e = value at the edge of the exhaust hole
m = minimum value

I. Introduction

VORTEX tubes of one form or another have been of interest to fluid dynamicists for some time. Applications such as the Ranque-Hilsch tube, cyclone separator, and, more recently, the MHD vortex power generator[1] and gaseous-core nuclear rocket[2] have provided the stimulus for research in this field. Analytical and experimental investigations of confined vortex flows have been numerous. The theoretical treatments have been concerned with the main body of rotating fluid and, for the most part, have been restricted to one-dimensional flow models (i.e., tangential and radial velocities being functions of radius only). Donaldson[3] examined the full Navier-Stokes equations under these assumptions and found a family of exact solutions. These exact solutions are not readily applicable to the flow in an actual vortex tube, however, because of their inability to satisfy boundary conditions imposed by the end walls and exhaust-hole geometry. Others[4, 5] have developed approximate theories in which the radial distributions of axial velocity are specified (rather arbitrarily) in order to satisfy conditions imposed by the exhaust ports. A notable exception is a study by Anderson[6] in which the laminar end-wall boundary-layer interaction problem was first treated.

Lewellen[7] has reviewed these studies and has clarified the mathematical foundation of the approximate solutions. In particular, he has shown that under certain circumstances (which are usually met experimentally) the one-dimensional hypothesis can yield a valid first approximation to the solution. In regions where this is the case, the axial velocity distribution is determined to the same degree of exactness by its boundary values. In an actual vortex tube, these are determined by the boundary layers on the end walls and by the location and geometry of the exit port (or ports), as just mentioned. Solutions based on arbitrarily specified axial velocity distributions have been reasonably successful in predicting the qualitative behavior of the measured tangential velocity distributions, numerical discrepancies being attributed usually to turbulence in the flow field.[4, 8, 9]

The boundary layers that are formed on the end walls of the vortex chamber have been studied previously without regard to their effect on the primary vortex flow that drives them. Boundary-layer growth on a finite disk under the influence of a vortex-like outer flow has been studied originally by Taylor[10] and more recently by Mack,[11] King,[12] Weber,[13] Rott,[14] and others. These studies, in which the external velocity distributions were specified functions of the radial coordinate, have demonstrated that such boundary layers are capable of transporting large quantities of fluid radially inward. This radial flow is coupled through the continuity equation to an axial flow, so that in fact it is the boundary-layer flow that determines, for the most part, the axial velocity distribution in a vortex tube.

For a fixed total flow through the tube, diversion of fluid into the boundary layers reduces the radial flow through the main body of the vortex and tends to weaken the vortex strength or circulation. In an actual vortex tube (such as pictured in Fig. 1), however, the boundary layers must at

Received February 26, 1964; revision received July 27, 1964. The authors wish to acknowledge the contributions of Jack Macki and Irene Wong of the Aerospace Corporation Computation and Data Processing Center for the programing and computation of data used in this paper.

* Staff Scientist, Laboratories Division. Member AIAA.
† Head, Fluid Dynamics Section, Laboratories Division. Member AIAA.
‡ Member of the Technical Staff, Laboratories Division. Member AIAA.

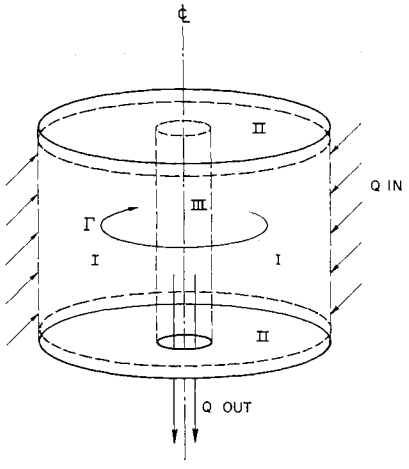

Fig. 1 Vortex tube geometry showing division of flow into the three regions described in the paper.

some point discharge their contents. If this process is accomplished in such a way as to return the boundary-layer fluid to the main flow before it has lost much of its angular momentum and before it is passed axially out of the tube, then (as is described in this paper) it is possible to maintain a near-constant circulation distribution in the vortex.

Mass flow may be caused to leave the boundary layer for two reasons. First, the boundary-layer theory itself indicates mass ejection when the external circulation distribution decreases with decreasing radius.[12] Second, certain discontinuities in the wall geometry, such as a circular step or the sharp edge of an exhaust orifice (i.e., regions where boundary-layer theory is not locally applicable), can also induce mass ejection. Experimental evidence of such boundary-layer mass ejection is plentiful[15–17]; typical examples are shown in Figs. 2 and 3 using a water vortex with dye injection. Figure 2 shows boundary-layer mass ejection in the vicinity of the exhaust-hole radius, resulting, most likely, from both mechanisms. Figure 3 illustrates the effect of a circular step in the end wall at approximately midradius. Mass ejection is again observed.

The full three-dimensional flow pattern in a vortex tube is thus the result of a complicated interaction between the primary vortex flow and the end-wall boundary layers. The purpose of the present paper is to study this interaction theoretically in order to demonstrate the unusual mutual influences exerted by the primary and secondary flows in right-cylindrical vortex tubes of the type illustrated in Fig. 1. The results are compared with experiments, and, as a corollary, certain observations are made concerning turbulence levels in confined vortex flows.

II. Description of Flow Model

An incompressible, constant viscosity fluid is assumed. For the purposes of the analysis the flow is considered divisible into three regions, as indicated in Fig. 1. It will be assumed that the ratio of volume flow to circulation is small so that in region I, the primary flow region, the tangential velocity is a function of radius only. Region II consists of the boundary layers on both top and bottom end walls, in which axial velocity gradients and therefore axial viscous stresses become significant. Region III, bounded by an imaginary cylinder of radius equal to that of the exhaust hole, includes the flow in the vicinity of the axis of the tube where both tangential and radial velocities vanish.

Appropriate solutions are employed in each of these regions, and a consistent flow picture is obtained by application of suitable matching conditions. The solution of Lewellen,[7] which determines the circulation distribution in terms of the stream function, is used in regions I and III. This solution becomes exact in the limit of large circulation and requires that the stream function be specified at the periphery of the applicable regions. The approximate boundary-layer solution of Rott[14] is used along the end walls, up to the edge of region III, to provide a second relationship between the stream function and circulation in the primary flow, thereby establishing the interaction. The

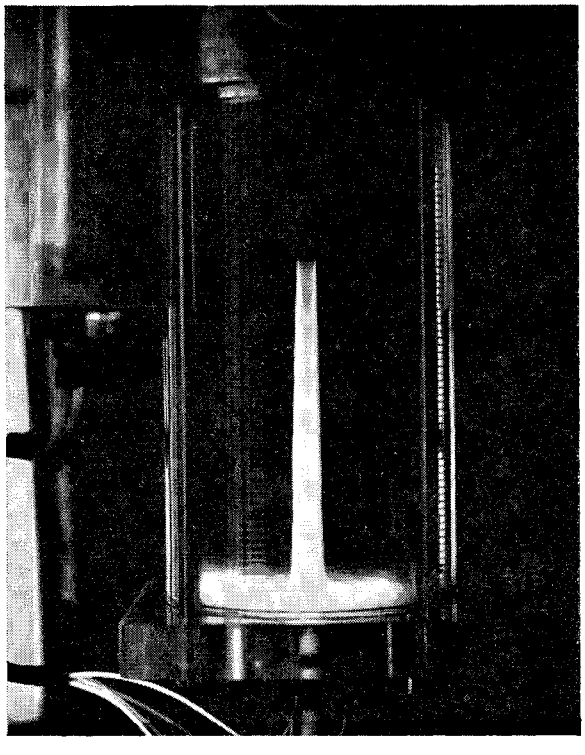

Fig. 2 Vortex flow visualization picture with dye injected into the boundary layer showing mass ejection in vicinity of exhaust radius.

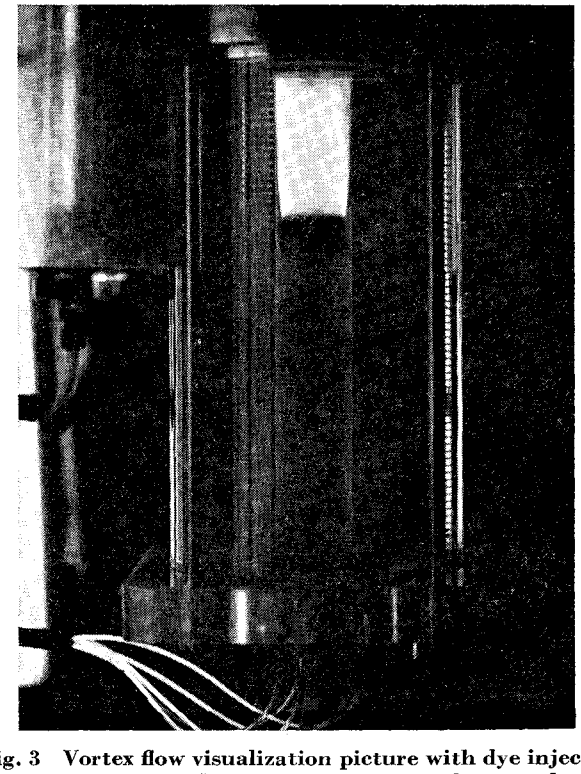

Fig. 3 Vortex flow visualization picture with dye injected into the boundary layer with a stepped-down end wall showing mass ejection in neighborhood of step.

mathematical framework is completed with the specification of the stream function in region III. Provision is included to allow the consideration of boundary-layer mass ejection due to the exhaust-hole discontinuity. Since little of a quantitative nature is known about this process at the present time, this phenomenon is treated parametrically. The fraction ζ of boundary-layer mass flow at the radius of the exhaust, which is returned to the main flow before leaving the tube, is introduced into the computational program and allowed to vary from zero to one. The complete set of equations is solved iteratively using a digital computer for a range of the governing parameters.

Before proceeding with the analysis, several comments are in order. First, the division of the flow into regions as indicated is not equivalent to the usual division of flows into a viscous boundary layer and an inviscid outer flow. In the present problem, the entire flow field is considered viscous; however, in the boundary layers, the axial velocity gradients predominate, whereas in regions I and III only the radial gradients are considered.

Second, the details of the flow in region III are oversimplified as a result of insufficient knowledge. Recirculation of fluid originating downstream of the exhaust hole, which frequently occurs along the axis of the vortex tube, has been neglected. This can be justified only by the belief that such a phenomenon does not strongly influence the velocity distributions in regions I and II.

Finally, a real and possibly important phenomenon is not considered at all in this paper, i.e., the boundary layer on the cylindrical-containing walls and the details of the jet-mixing region if the vortex is driven by tangential fluid injection, as is commonly the case. These effects may influence the end-wall boundary-layer growth and will certainly make the determination of the peripheral circulation difficult in an actual experiment. For the present purposes, however, it is assumed that the outer cylinder is rotating and porous so that such questions may be avoided.

III. Derivation of the Interaction Equations

Consider a cylindrical coordinate system, r,θ,z, with associated velocity components u, v, w. The continuity and Navier-Stokes equations in these coordinates for an incompressible fluid with constant viscosity are

$$\frac{\partial(ru)}{\partial r} + \frac{\partial(rw)}{\partial z} = 0 \tag{1}$$

$$u\frac{\partial u}{\partial r} + w\frac{\partial u}{\partial z} - \frac{v^2}{r} = -\frac{1}{\rho}\frac{\partial p}{\partial r} + \nu\left(\frac{\partial^2 u}{\partial r^2} + \frac{1}{r}\frac{\partial u}{\partial r} - \frac{u}{r^2} + \frac{\partial^2 u}{\partial z^2}\right) \tag{2}$$

$$u\frac{\partial v}{\partial r} + w\frac{\partial v}{\partial z} + \frac{uv}{r} = \nu\left(\frac{\partial^2 v}{\partial r^2} + \frac{1}{r}\frac{\partial v}{\partial r} - \frac{v}{r^2} + \frac{\partial^2 v}{\partial z^2}\right) \tag{3}$$

$$u\frac{\partial w}{\partial r} + w\frac{\partial w}{\partial z} = -\frac{1}{\rho}\frac{\partial p}{\partial z} + \nu\left(\frac{\partial^2 w}{\partial r^2} + \frac{1}{r}\frac{\partial w}{\partial r} + \frac{\partial^2 w}{\partial z^2}\right) \tag{4}$$

where the $\partial/\partial t$ and $\partial/\partial\theta$ terms have been eliminated by assuming that the flow is steady and axisymmetric.

The axisymmetric stream function ψ is defined so that Eq. (1) is everywhere satisfied:

$$u = \frac{1}{r}\frac{\partial\psi}{\partial z} \qquad w = -\frac{1}{r}\frac{\partial\psi}{\partial r} \tag{5}$$

In addition, the dimensionless coordinates $\eta = (r/r_0)^2$ and $\xi = z/l$ and the quantities $Q = ur$ and $\Gamma = vr$ are introduced.

Lewellen[7] showed that $\partial\Gamma/\partial\xi$ was of order ϵ, where

$$\epsilon = (\psi_0/\Gamma_0 r_0)^2 \tag{6}$$

Therefore, in regions where the ratio of stream function to circulation is small, Γ may be considered independent of z, to order ϵ. Further, examination of Eq. (3) shows that, when v is independent of z, the radial velocity u must also be independent of z (unless Γ = const). In this case, Eq. (3) reduces to an ordinary, linear differential equation for Γ in terms of u and ν:

$$r^2\frac{d}{dr}\left(\frac{1}{r}\frac{d\Gamma}{dr}\right) - \frac{ur}{\nu}\frac{d\Gamma}{dr} = 0 \tag{7}$$

The most general form of ψ, consistent with the condition that u be independent of z, is

$$\psi = Q_0 l[\xi f(\eta) + F(\eta)] \tag{8}$$

so that

$$u = \frac{Q_0}{r}f \qquad w = -\frac{2Q_0 l}{r_0^2}\left(\frac{z}{l}f' + F'\right)$$

Lewellen[7] has further shown that, since the equation that determines ψ is of order ϵ, to this order then the functions f and F remain to be determined by the boundary conditions.

In terms of f, η, and the radial Reynolds number $Re_r = Q_0/\nu$, Eq. (7) may be rewritten:

$$2\eta\Gamma'' - Re_r f\Gamma' = 0 \tag{9}$$

The functions ψ and Γ as defined by Eqs. (8) and (9) were shown by Lewellen[7] to be the zeroth-order terms in a series expansion solution of Eqs. (1–4), in powers of ϵ.

If the axial and tangential velocities are of the same order in region III, then in this region the ϵ expansion given in Ref. 7 is not strictly valid. This question is quite complicated but is treated in detail in Ref. 18 where it is shown that it is still possible to carry out a consistent expansion in u/v, which almost always remains a small parameter. In such an expansion, the leading term in Γ is still a function of r only and may be determined by an equation similar to Eq. (9), which depends on the boundary values of ψ:

$$2\eta\Gamma'' - Re_r f\Gamma' = -4Re_r\frac{\eta F'}{\Gamma}\left[F'''f - F'f'' - \frac{2}{Re_r}(2F''' + \eta F'''')\right]\left(\frac{w}{v}\right)_e^2 \tag{10}$$

If precise values of ψ could be obtained on the boundaries of region III, then Eq. (10) would yield an accurate description of Γ even for $(w/v)_e$ of order one. However, for the idealized stream function that will be used in this study, the right-hand side of Eq. (10) is identically zero and the equation reduces to Eq. (9).

Applying the boundary conditions $\Gamma = 0$ at $\eta = 0$ and $\Gamma = \Gamma_0$ at $\eta = 1$, Eq. (9) may be integrated to give

$$\frac{\Gamma}{\Gamma_0} = c_1\int_0^\eta \exp\left[\frac{Re_r}{2}\int_0^\eta\frac{f(\eta)}{\eta}\,d\eta\right]d\eta \tag{11}$$

where

$$c_1 = \left\{\int_0^1 \exp\left[\frac{Re_r}{2}\int_0^\eta\frac{f(\eta)}{\eta}\,d\eta\right]d\eta\right\}^{-1}$$

Thus, with a given value of the radial Reynolds number and the radial distribution of f, the circulation distribution is uniquely determined.

It should be noted at this point that only f enters in the determination of Γ. That is, only that portion of the axial flow which is coupled to the radial flow through the continuity relationship plays a role.

The f distribution, or equivalently the distribution of radial velocity through regions I and III, will be determined by consideration of the end-wall boundary-layer flow. Since it is assumed that the boundary-layer mass flow grows from

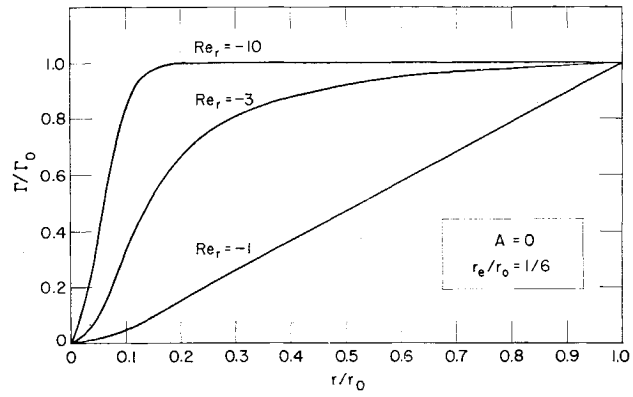

Fig. 4 Circulation distributions as a function of radius for $A = 0$.

zero at r_0, any increase (or decrease) in the radial flow in the boundary layers must result in a corresponding decrease (or increase) in the radial flow through the primary vortex region. Thus (in region I),

$$f = 1 - (2Q_{BL}/Q_0 l) \tag{12}$$

where

$$Q_{BL} = \int_0^{\delta} rudz$$

There have been several analyses of the end-wall boundary-layer region.[11–14] For the present study, the results of the turbulent analysis of Rott[14] will be used. This is chosen because, at the tangential Reynolds numbers ordinarily encountered in vortex tubes, the boundary layers are most likely turbulent, and although Rott's analysis yields the simplest expression for the mass flow in the boundary layer, the results agree quite favorably with those of other, more complicated approaches. Assuming that the turbulent shear components are proportional to the squares of the respective velocity components and that the coefficient of friction so defined is constant, Rott, using a momentum-integral approximation, expressed the volume flow in the boundary layer in terms of the Γ distribution of the external flow as follows:

$$Q_{BL} = -\alpha c \Gamma^{\alpha-1} \int_0^x \Gamma^{2-\alpha} dx \tag{13}$$

where $x = r_0 - r$, α is a velocity-profile shape parameter, and c is the coefficient of friction. Following Rott, the values

$$\alpha = 5 \qquad c = 0.027(Re_t)^{-1/5} \tag{14}$$

will be used for this study.

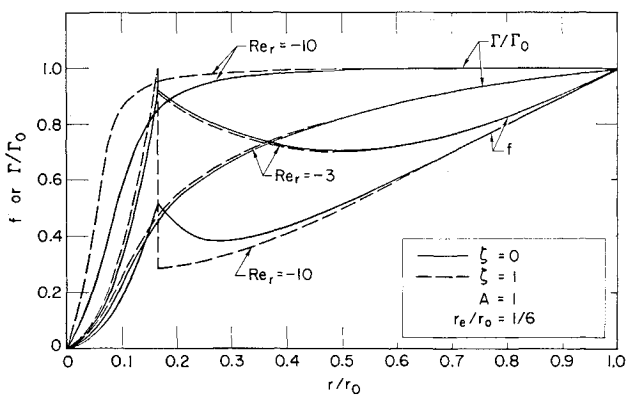

Fig. 5 Circulation and stream function distributions as a function of radius for $A = 1$.

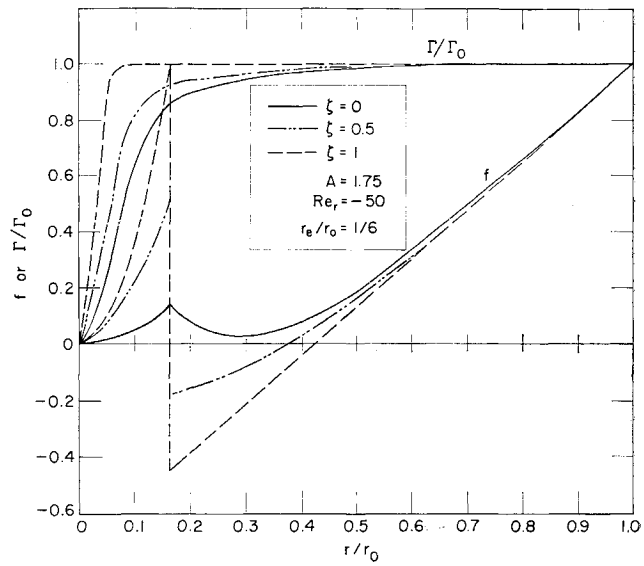

Fig. 6 Circulation and stream function distributions as a function of radius for $A = 1.75$ and $Re_r = -50$.

The specification of f in region III is not quite so straightforward. As mentioned previously, the discontinuity at the edge of the exit hole (assumed here to be a sharp-edged orifice) produces local mass ejection from the boundary layer. The fraction of the boundary-layer mass flow that is ejected and ultimately finds its way back into the primary flow is as yet undetermined. Furthermore, the questions of recirculatory flow along the axis and the validity of the boundary-layer analysis near the axis contribute to the difficulty of specifying f in detail in region III. Fortunately, as far as the calculation of the circulation is concerned, only the integral of f appears in Eq. (11). Thus, Γ should be insensitive to the details of the axial velocity distribution (as long as v is independent of z).

It will be assumed then that a certain fraction ζ of the boundary-layer volume flow at r_e (the radius of the exit hole) is ejected and returned to the primary flow to be redistributed into radial flow uniformly over the length of the tube. The representation of this boundary-layer mass ejection by a discontinuous change in f is, of course, an idealization of the actual phenomena illustrated in Figs. 2 and 3. The quantity ζ will be considered parametrically in the computations, and its effect on the Γ and f distributions will be assessed. In addition, inside the radius of the ex-

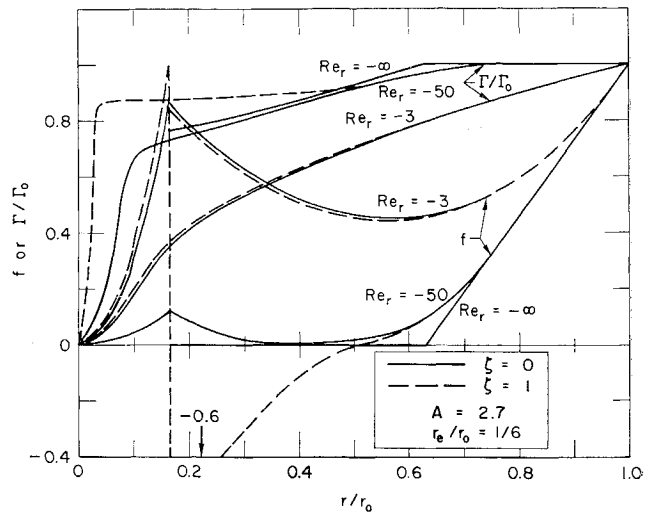

Fig. 7 Circulation and stream function distributions as a function of radius for $A = 2.7$.

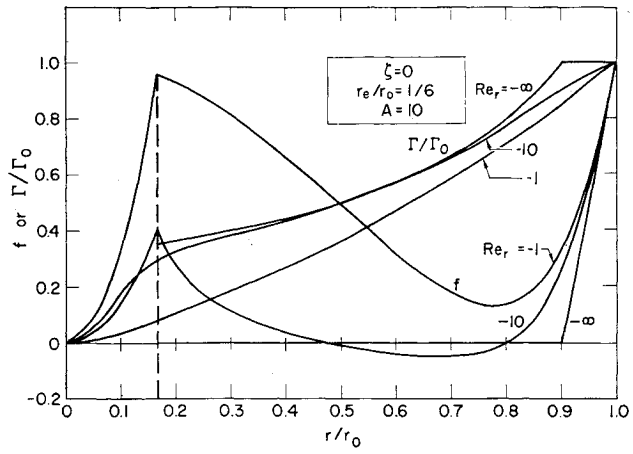

Fig. 8 Circulation and stream function distributions as a function of radius for $A = 10$.

haust, the simplest possible assumption will be made, namely, that the radial velocity falls to zero at $r = 0$ linearly with r. Under these conditions,

$$f = \left[1 - (1 - \zeta)\frac{2Q_{BL}(r_e)}{Q_0 l}\right]\frac{r^2}{r_e^2} \tag{15}$$

when $r \leq r_e$.

Considering Eqs. (12–15), f may be written as

$$f = 1 - A\left[\frac{\Gamma(\eta)}{\Gamma_0}\right]^4 \int_\eta^1 \left[\frac{\Gamma_0}{\Gamma(\eta)}\right]^3 \frac{d\eta}{2(\eta)^{1/2}} \qquad 1 \geq \eta > \eta_e \tag{16}$$

$$f = \frac{\eta}{\eta_e}\left\{1 - (1 - \zeta)A\left[\frac{\Gamma(\eta_e)}{\Gamma_0}\right]^4 \int_{\eta_e}^1 \left[\frac{\Gamma_0}{\Gamma(\eta)}\right]^3 \frac{d\eta}{2(\eta)^{1/2}}\right\} \qquad 0 \leq \eta \leq \eta_e$$

where

$$A = -\frac{0.27}{(Re_l)^{1/5}}\left(\frac{\Gamma_0 r_0}{Q_0 l}\right) = \frac{2c\alpha}{\epsilon^{1/2}} \tag{17}$$

Equations (11) and (16) determine f and Γ as functions of the radius and the parameters Re_r, A, r_e/r_0, and ζ. These equations have been solved iteratively using a digital computer for ranges of the governing parameters, and the results are presented and discussed in the next section.

IV. Discussion of Results

The quantity A characterizes the boundary-layer interaction since it is a measure of the fraction of the total mass flow that passes through the boundary layer. If Γ were constant and equal to Γ_0 for all r, then it can be seen from Eqs. (13, 14, and 17) that A would be equal to the fraction of the total mass flow in the boundary layers at $r = 0$. Also, from Eq. (17) it is seen that $A \sim 1/\epsilon^{1/2}$, so that small values of ϵ ordinarily correspond to large values of the boundary-layer interaction parameter. Thus, it is precisely in the regime where Γ is independent of z that the end-wall boundary-layers will play a significant role in the determination of the radial Γ distribution.

An interesting exception occurs in the limit of A going to zero as a result of frictionless, or suitably rotating, end walls (i.e., not because ϵ becomes large). In this case, the present problem becomes identical with that considered by Einstein and Li.[5] This solution is shown in Fig. 4 for three values of the radial Reynolds number and $r_e/r_0 = \frac{1}{6}$.

Another interesting limiting case, which may be solved analytically, occurs when $Re_r \to -\infty$. This case has been

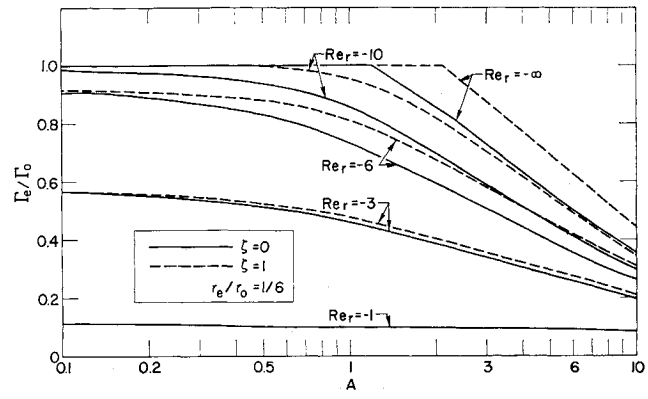

Fig. 9 Circulation at the edge of the exhaust hole as a function of A for constant Re_r.

solved in the Appendix. In this limit, the circulation distribution remains constant for $A < 0(1)$. For $A > 0(1)$, the circulation remains constant with decreasing radius from r_0 until all of the flow reaches the end-wall boundary layers. Between this radius and the edge of the exhaust hole the total radial flow remains in the boundary layers, and the circulation distribution is that required to drive this boundary-layer flow.

Results of the digital computer solutions for Γ and f distributions corresponding to various combinations of the governing parameters are shown in Figs. 5–8. All of these results were obtained for a constant value of $r_e/r_0 = \frac{1}{6}$. The successive figures correspond to increasing values of A. Values of radial Reynolds number have been chosen so that results representative of the distributions obtainable are presented. In most of these figures, curves are plotted only for $\zeta = 0$ and $\zeta = 1$, since results for intermediate values may be easily inferred from those presented. In Fig. 6, the curve for $\zeta = 0.5$ is also presented, indicating a rather uniform variation of the distributions with ζ between the extremes of zero and one. Results of the analytical solution of the Appendix for $Re_r = -\infty$ are included in Figs. 7 and 8.

The curves illustrate that when $A \leq 1$ the effect of the boundary-layer interaction is relatively small. The same is true when $|Re_r|$ is small regardless of the value of A. In both of these areas, of course, the influence of ζ is also small. For slightly larger values of A, the boundary-layer interaction begins to exert a considerable influence, especially at the higher values of $|Re_r|$. The effect of ζ also becomes

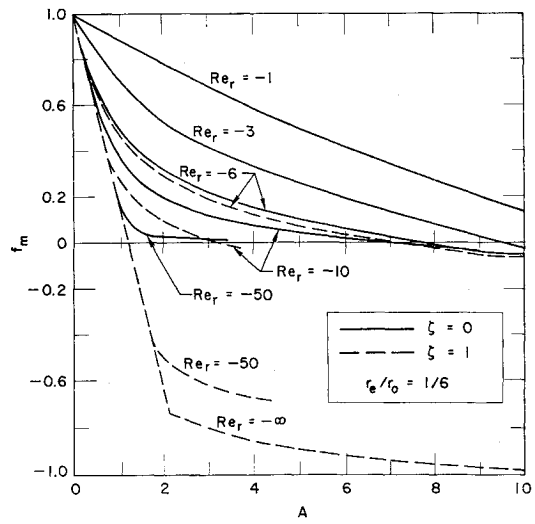

Fig. 10 Minimum mass flow in the primary flow region as a function of A for constant Re_r.

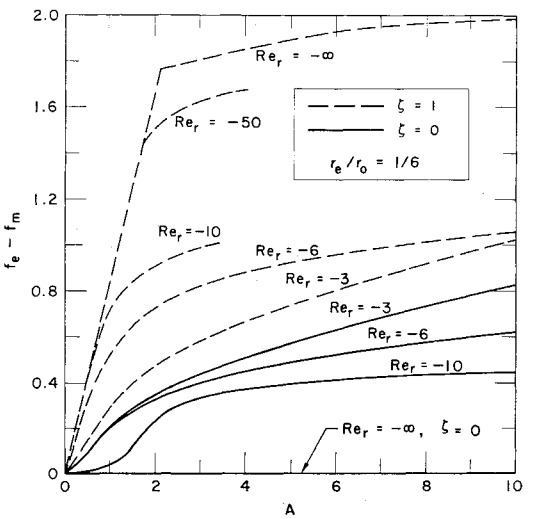

Fig. 11 Amount of fluid returned by the boundary layers to the primary flow as a function of A for constant Re_r.

more pronounced here. A value of $\zeta = 1$ causes the circulation distribution to stay closer to a constant and results in increases of Γ_e/Γ_0 of up to 20%. Its influence on the mass-flow distribution is more profound (as seen in Figs. 6 and 7), resulting in negative values of f, which implies that the boundary-layer mass flow is locally greater than the total through-flow so that radial outflow must exist in the primary-flow region. It is interesting to note that, in spite of this excess mass flow in the boundary layers, the Γ distribution remains essentially constant.

At still larger values of the interaction parameter, the Γ distribution decreases faster (see Fig. 8), and the theoretical results for infinite Reynolds number are approximated closely by those for more moderate Reynolds numbers.

In order to characterize the effect of the interaction in a simple way, the value of Γ_e/Γ_0 is plotted in Fig. 9 as functions of A and Re_r for $r_e/r_0 = \frac{1}{6}$. This curve also illustrates the influence of ζ. It is seen that, for $\zeta = 0$, values of Γ_e/Γ_0 begin to depart from one when $A > 1.2$, even for infinite Reynolds number. For $\zeta = 1$, this departure is delayed until $A > 2.2$.

The mass-flow distributions are characterized by the minimum value of f (designated f_m) and the amount of fluid that is returned by the boundary layers to the primary flow ($f_e - f_m$). These distributions are plotted in Figs. 10 and 11.

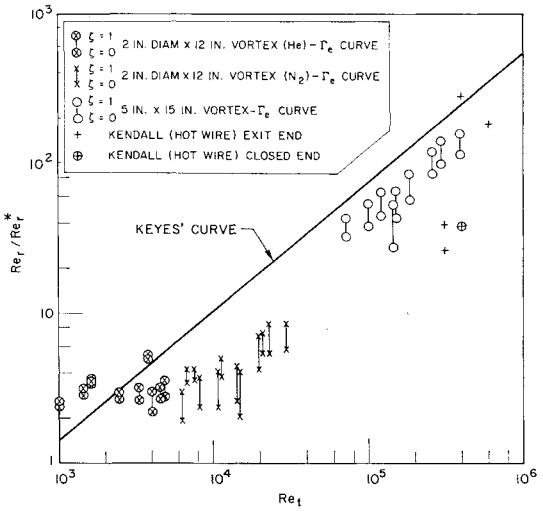

Fig. 12 The ratio of laminar radial Reynolds number to effective turbulent radial Reynolds number as a function of tangential Reynolds number.

Negative values of f_m indicate reverse flow regions in the primary flow.

In order to assess the influence of r_e on the Γ and f distributions, solutions were obtained for values of r_e/r_0 other than $\frac{1}{6}$. These results are contained in Ref. 19.

The effects of compressibility are also treated in Ref. 19 by consideration of an isothermal flow. It is concluded that the present results are accurate for most practical applications.§

V. Comparison with Experiment and Comments Regarding Turbulence

It has been traditional to compare experimental results and theory by matching the measured circulation distributions (deduced from static pressure measurements) with the analytical predictions. In all cases, it has been found that circulation profiles could be matched only when the measured laminar radial Reynolds number was much higher than its theoretical counterpart. As mentioned in the Introduction, previous investigations of vortex flow in tubes were based on one-dimensional flow models (equivalent to setting $A = 0$ in the present theory) and tended to ascribe discrepancies between measured and theoretically computed circulation profiles to the presence of turbulence in the flow field. It was assumed that the turbulence produced a large "eddy viscosity" that in turn resulted in a reduced radial Reynolds number. The ratio of the theoretically deduced "effective" radial Reynolds number to the actual radial Reynolds number based on a laminar viscosity was used as a measure of the turbulence level in the tube. Thus, Keyes,[8] for example, was able to arrive at a correlation between apparent turbulence level and the tangential peripheral Reynolds number of the flow.

Subsequently, Kendall[16] and others pointed out the significance of the end-wall boundary-layer interaction and suggested that the reduction in Γ distribution, which had been attributed to turbulence, may indeed be explainable largely or wholly by the three-dimensional boundary-layer interaction. It was argued that diversion of flow into the boundary layers reduced the radial Reynolds number in the primary flow, thus accounting for the reduced values of Γ/Γ_0.

As the present study shows, however, when Γ/Γ_0 begins to depart from one, the boundary-layer growth slows down and finally reverses, resulting in fluid being returned to the primary flow. Since only a fraction of the fluid's angular momentum is lost in the boundary layer (on the average), mass ejection from the boundary layer tends to support the angular momentum distribution, retarding its further decline. Finite values of ζ contribute further to this trend, resulting, as has been seen, in the requirement that A be greater than 1.2 for $\zeta = 0$ (or 2.2 if $\zeta = 1$) before any significant degradation of the Γ profile occurs because of the boundary-layer interaction.

In order to determine whether three-dimensionality can indeed explain all or part of the experimentally observed velocity distributions, some new experiments were conducted, using two different vortex chambers. Somewhat modified versions of the apparatus described by Rosenzweig[20] and by Grabowsky and Rosenzweig[21] were used. The vortex tubes were similar to those employed by Keyes, having rows of discrete jets injecting tangentially at the periphery and a central exhaust hole at one end. One tube was 2-in. i.d. × 12 in. long and was operated in a low-density (low Reynolds number) regime with either nitrogen or helium as the working fluid. The other tube was 5-in. i.d. × 15 in. long and was operated with nitrogen only. Mass-flow measurements and radial pressure distributions were taken. The latter were used to infer tangential velocity distributions. It was pos-

§ An independent analysis by Anderson[22] has treated the compressibility effects in more detail but with similar conclusions.

sible, therefore, to calculate A, Γ_e, and the laminar radial and tangential Reynolds numbers from the measured quantities.

In comparing the normalized values of Γ_e with those predicted by the present theory for the same values of A and Re_r, it was found that the experimental values were consistently lower, the discrepancy being larger for higher tangential Reynolds numbers. Thus, the trends indicated by the one-dimensional analyses were still present.

Assuming that the theory adequately represents the three-dimensional interaction, it must be concluded that end-wall boundary-layer effects alone cannot explain the relatively weak vortices observed in experiments. In the authors' opinion it is most probable that the discrepancy is due to the presence of turbulence in the experimental flow field.

If it is assumed that the effects of turbulence can be treated theoretically by the introduction of a spatially constant turbulent "eddy viscosity" and suitably time-averaged velocity components (as is traditional in turbulent analyses), then the present theory remains valid if the radial Reynolds number is replaced by an "effective" Reynolds number based on the eddy viscosity. This hypothesis is certainly a questionable one for the present flow configuration because of the strong radial gradients and the likelihood that the turbulent fluctuations are highly anisotropic. Nevertheless, because of its simplicity, it has been used in the one-dimensional analyses and will be pursued further here for comparison.

The experiments just described were used in conjunction with the theory to infer a value of effective radial Reynolds number (Re_r*). Results are shown in Fig. 12 as a ratio of actual to "effective" radial Reynolds number vs tangential Reynolds number based on tube radius. A spread is indicated for each test point, the upper bound corresponding to $\zeta = 1$ and the lower to $\zeta = 0$. Also shown are several actual measurements of turbulence intensity made by Kendall[16] using a hot-wire anemometer and Keyes' least-squares line, which was fitted to data reduced using the one-dimensional hypothesis.[8] Values of A in the present experiments varied from 0.6 to 1.5, and Re_r ranged from 12 to several thousand. Calculations indicate that values of A of order one were also representative of Keyes' experiments. The comparison shown in Fig. 12 indicates that early estimates of turbulence levels in jet-driven vortices, even though based on one-dimensional flow models, are not far from those arrived at after consideration of three-dimensional effects.

VI. Conclusions

The equations governing the interaction between the primary flow and end-wall boundary layers in a vortex tube have been presented and solved iteratively on a digital computer. The controlling parameters include a boundary-layer interaction parameter A representing a measure of the mass fraction diverted to the boundary layers, the radial Reynolds number, and a parameter ζ representing the boundary-layer mass ejection occurring as a result of the geometrical discontinuity existing at the exhaust-hole radius. Circulation and mass-flow distributions are presented, illustrating the variety of results obtainable in the different flow regimes. Over-all results are characterized by the values of Γ_e/Γ_0, the circulation ratio at the exhaust radius, and f_m, the minimum mass flow in the primary flow region.

The results show that, if $A < 1$, the effect of the boundary layer interaction on the circulation distribution is small. The same is true if $|Re_r|$ is of order one, regardless of A. As A increases, the effect is more pronounced, the interaction producing a reduced Γ_e/Γ_0 and f_m. A variation of ζ from zero to one produces a maximum increase of approximately 20% in Γ_e/Γ_0, but can have a profound effect on f_m, causing negative values (i.e., reverse flow) to occur in some instances. It has been shown that in some cases it is possible to have an excess of flow in the boundary layer (i.e., $f_m < 0$) while Γ/Γ_0 remains close to unity.

The theoretical results have been compared with experiments by matching experimental and theoretical circulation profiles and thereby determining a ratio of actual (laminar) to "effective" radial Reynolds number. By comparison with previous results, it has been concluded that turbulence levels in jet-driven vortex flows are not appreciably less than those based on one-dimensional model assumptions.

Appendix: Analytic Solution for Infinite Reynolds Number

An analytic solution to Eqs. (11) and (16) is possible in the limit of $Re_r \to -\infty$. From Eq. (9) it is seen that, in order to have a finite value of f in this limit, either an infinity or a zero in Γ' is required. Conversely, any Γ distribution is possible when $f = 0$, since the product $Re_r f$ is then indeterminate. Therefore, it is evident that in this limit Γ will remain constant at large radii until all of the flow reaches the end-wall boundary layers, i.e., until $f = 0$. Proceeding inward from this point, all the flow will remain in the boundary layers, and the circulation will distribute itself in just such a way as to keep $f = 0$. This distribution may be found by writing Eq. (13) in differential form

$$(d/dr)Q_{BL}\Gamma - \alpha Q_{BL}(d\Gamma/dr) = \alpha c\Gamma^2 \tag{A1}$$

For $Q_{BL} = \text{const}$, this reduces to

$$\frac{1}{\Gamma^2}\frac{d\Gamma}{dr} = \frac{\alpha c}{Q_{BL}(1-\alpha)} \tag{A2}$$

Equation (A2) integrates to

$$\frac{\Gamma_0}{\Gamma} = \frac{A}{(1-\alpha)(1-f)}\frac{r}{r_0} + c_2 \tag{A3}$$

in terms of previously defined dimensionless parameters. The constant c_2 is evaluated by the condition that $\Gamma/\Gamma_0 = 1$ at $r = \hat{r}$, the radius at which f first reaches zero. For $r > \hat{r}$, from Eqs. (12) and (13)

$$f = 1 - A[1 - (r/r_0)] \tag{A4}$$

Therefore,

$$\hat{r}/r_0 = 1 - 1/A \tag{A5}$$

From Eq. (A5) and the condition that $\Gamma/\Gamma_0 = 1, f = 0$ at $\hat{r} = \hat{r}$, Eq. (A3) reduces to

$$\frac{\Gamma}{\Gamma_0} = \frac{\alpha - 1}{\alpha - 2 + A[1 - (r/r_0)]} \qquad r < \hat{r} \tag{A6}$$

For $\zeta = 0$, the solution for the Γ distribution in the limit of $Re_r \to -\infty$ is $\Gamma = \Gamma_0$ for $r > \hat{r}$ and is given by Eq. (A6) for $r_e < r < \hat{r}$. Inside the exhaust radius it is undetermined.

The solution for $\zeta \neq 0$ is slightly different. At the radius of the exhaust, flow is forced out of the boundary layer so that $f > 0$ when $r < r_e$. Thus Γ' must be zero here from Eq. (9). Furthermore, differentiation of Eq. (11) indicates that Γ' must remain zero for $r > r_e$ until

$$\int_0^{\eta} \frac{f}{\eta}\, d\eta \leq 0 \tag{A7}$$

This in turn requires f to be negative in some region outside the radius of the exhaust. Thus, for $\zeta \neq 0$, Eq. (A6) applies only to $r > r^*$, with r^* defined so that

$$\int_0^{\eta^*} \frac{f}{\eta}\, d\eta = 0 \tag{A8}$$

To complete Eq. (A8), f is given by

$$f = (\eta/\eta_e)[1 + (1 - \zeta)(f_e - 1)] \qquad \eta < \eta_e$$

$$f = A(\Gamma_e/\Gamma_0)[\eta^{1/2} - (\eta^*)^{1/2}] \qquad \eta_e < \eta < \eta^* \tag{A9}$$

Equations (A8) and (A9) yield an algebraic equation relating Γ_e and η^*:

$$1 - (1 - \zeta)\left\{1 - A\frac{\Gamma_e}{\Gamma_0}[\eta^{1/2} - (\eta^*)^{1/2}]\right\} = A\frac{\Gamma_e}{\Gamma_0} \times \left\{(\eta^*)^{1/2} \ln\frac{\eta^*}{\eta_e} - 2[(\eta^*)^{1/2} - (\eta_e)^{1/2}]\right\} \tag{A10}$$

A second equation relating Γ_e and η^* is obtained from Eq. (A6), which is valid at η^*:

$$\frac{\Gamma_e}{\Gamma_0} = \frac{\alpha - 1}{\alpha - 2 + A[1 - (\eta^*)^{1/2}]} \tag{A11}$$

Equations (A10) and (A11) must be solved simultaneously to obtain Γ_e and η^*. Results for Γ_e/Γ_0 are included in Fig. 9.

References

[1] Lewellen, W. S. and Grabowsky, W. R., "Nuclear space power systems using magnetohydrodynamic vortices," ARS J. **32,** 693–700 (1962).

[2] Kerrebrock, J. L. and Meghreblian, R. V., "Vortex containment for the gaseous fission rocket," J. Aerospace Sci. **28,** 710–724 (1961).

[3] Donaldson, C. duP. and Sullivan, R. D., "Behavior of solutions of the Navier-Stokes equations for a complete class of viscous vortices," *Proceedings of the Heat Transfer and Fluid Mechanics Institute* (Stanford University Press, Stanford, Calif., 1960), pp. 16–30.

[4] Deissler, R. G. and Perlmutter, M., "An analysis of the energy separation in laminar and turbulent compressible vortex flows," *Proceedings of the Heat Transfer and Fluid Mechanics Institute* (Stanford University Press, Stanford, Calif., 1958), pp. 40–53.

[5] Einstein, H. A. and Li, H., "Steady vortex flow in a real fluid," *Proceedings of the Heat Transfer and Fluid Mechanics Institute* (Stanford University Press, Stanford, Calif., 1951), pp. 33–43.

[6] Anderson, O., "Theoretical solutions for the secondary flow on the end wall of a vortex tube," UAC Research Labs. Rept. R-2494-1, United Aircraft Corp. (November 1961).

[7] Lewellen, W. S., "A solution for three-dimensional vortex flows with strong circulation," J. Fluid Mech. **14,** 420–432 (1962).

[8] Keyes, J. J., Jr., "An experimental study of flow and separation in vortex tubes with application to gaseous fission heating," ARS J. **9,** 1204–1210 (1961).

[9] Ragsdale, R. G., "NASA research on the hydrodynamics of the gaseous vortex reactor," NASA TN-D-288 (June 1960).

[10] Taylor, G. I., "The boundary layer in the converging nozzle of a swirl atomizer," Quart. J. Mech. Appl. Math. **3,** 129–139 (1950).

[11] Mack, L. M., "Laminar boundary layer on a disk of finite radius in a rotating flow, Part I," Jet Propulsion Lab. Rept. TR-32-224 (May 1962).

[12] King, W. S., "Momentum integral solutions for the laminar boundary layer on a finite disk in a rotating flow," Aerospace Corp. Rept. ATN-63(9227)-3 (June 1963).

[13] Weber, H. E., "Boundary layer inside a conical surface due to swirl," J. Appl. Mech. **23,** 587–592 (1956).

[14] Rott, N., "Turbulent boundary layer development on the end walls of a vortex chamber," Aerospace Corp. Rept. ATN-62(9202)-1 (July 1962).

[15] Rosenzweig, M. L., Ross, D. H., and Lewellen, W. S., "On secondary flows in jet-driven vortex tubes," J. Aerospace Sci. **29,** 1142 (1962).

[16] Kendall, J. M., Jr., "Experimental study of a compressible viscous vortex," Jet Propulsion Lab. Rept. TR-32-290 (June 1962).

[17] Ross, D. H., "An experimental study of secondary flow in jet-driven vortex chambers," Aerospace Corp. Rept. ATN-64(9227)-1 (January 1964).

[18] Lewellen, W. S., "Three-dimensional viscous vortices in incompressible flow," Ph.D. Dissertation, Univ. of California at Los Angeles (1964).

[19] Rosenzweig, M. L., Lewellen, W. S., and Ross, D. H., "Confined vortex flows with boundary-layer interaction," Aerospace Corp. Rept. ATN-64(9227)-2 (February 1964).

[20] Rosenzweig, M. L., "Summary of research in the field of advanced nuclear propulsion, semiannual technical report," Aerospace Corp. Rept. TDR-930(2210-14)-TR-1 (March 1962).

[21] Grabowsky, W. R. and Rosenzweig, M. L., "Advanced propulsion, semiannual technical note," Aerospace Corp. Rept. ATN-63(9227)-2 (April 1963).

[22] Anderson, O., "Theoretical effect of Mach number and temperature gradient on primary and secondary flows in a jet-driven vortex," UAC Research Labs. Rept. RTD-TDR-63-1098, United Aircraft Corp. (November 1963).